Original Article

JCBFM

Journal of Cerebral Blood Flow & Metabolism
0(0) 1–9

DOI: 10.1177/0271678X20924549
journals.sagepub.com/home/jcbfm
SAGE

Integrating regional perfusion CT information to improve prediction of infarction after stroke

Julian Klug[1,2,*], Elisabeth Dirren[1,*], Maria G Preti[2,3], Paolo Machi[3], Andreas Kleinschmidt[1], Maria I Vargas[3], Dimitri Van De Ville[2,3] and Emmanuel Carrera[1]

Abstract

Physiological evidence suggests that neighboring brain regions have similar perfusion characteristics (vascular supply, collateral blood flow). It is largely unknown whether integrating perfusion CT (pCT) information from the area surrounding a given voxel (i.e. the receptive field (RF)) improves the prediction of infarction of this voxel. Based on general linear regression models (GLMs) and using acute pCT-derived maps, we compared the added value of cuboid RF to predict the final infarct. To this aim, we included 144 stroke patients with acute pCT and follow-up MRI, used to delineate the final infarct. Overall, the performance of GLMs to predict the final infarct improved when using RF for all pCT maps (cerebral blood flow, cerebral blood volume, mean transit time and time-to-maximum of the tissue residual function (Tmax)). The highest performance was obtained with Tmax (glm(Tmax); AUC $= 0.89 \pm 0.03$ with RF vs. 0.78 ± 0.02 without RF; $p < 0.001$) and with a model combining all perfusion parameters (glm(multi); AUC 0.89 ± 0.02 with RF vs. 0.79 ± 0.02 without RF; $p < 0.001$). These results suggest that prediction of infarction improves by integrating perfusion information from adjacent tissue. This approach may be applied in future studies to better identify ischemic core and penumbra thresholds and improve patient selection for acute stroke treatment.

Keywords

Machine learning, prediction, perfusion imaging, receptive field, stroke

Received 12 December 2019; Revised 25 February 2020; Accepted 30 March 2020

Introduction

Early and accurate prediction of the final infarct is crucial for the management of acute stroke patients. The initial perfusion imaging performed in most emergency wards is used to determine the salvageable brain tissue and estimate the final infarct. Perfusion-based infarct prediction is mostly performed for each voxel of interest (VOI) independently. However, it is likely that the fates of neighboring VOIs are closely interdependent, as they share similar physiological characteristics such as vascular supply and collateral blood flow. It remains largely unknown whether including acute perfusion imaging information from tissues adjacent to a given VOI improves the prediction of the final infarct. Magnetic resonance imaging (MRI) studies using machine learning methods such as artificial neuronal networks[1] and convolutional neural networks[2] that implicitly take into account spatial information from imaging data, suggest that adjacent perfusion information improves the prediction of outcome for a given VOI. However, these multi-parametric non-linear

[1]Stroke Research Group, Department of Clinical Neurosciences, University Hospital and Faculty of Medicine, Geneva, Switzerland
[2]Medical Imaging Processing Laboratory, Institute of Bioengineering, Ecole Polytechnique Fédérale de Lausanne (EPFL), Lausanne, Switzerland
[3]Division of Neuroradiology, University Hospital and Faculty of Medicine, Geneva, Switzerland

*These authors contributed equally to this work.

Corresponding author:
Emmanuel Carrera, Head, Stroke Center, Hôpitaux Universitaires Genève and Faculty of Medicine, 4, Rue Gabrielle Perret-Gentil, Geneva 1211, Switzerland.
Email: emmanuel.carrera@hcuge.ch

models remain difficult to implement in clinical practice due to the high computational overhead and conclusions from previous studies are limited by the low number of subjects and the size of voxels. Moreover, these models have been developed on perfusion and diffusion MRI datasets, leaving the benefit of including regional information in perfusion CT models largely unknown.

In this study, we investigated, in a large cohort of acute stroke patients, whether integrating acute perfusion CT information from neighboring VOI improves the performance of different models to predict the final infarct. To this aim, we developed a general linear model (GLM) integrating regional information based on the concept of "receptive fields" (RF).[3,4] We defined receptive fields as concentric cubes of different volumes around each voxel of CT perfusion maps. We systematically investigated RF of increasing sizes to determine to which extent the surrounding perfusion status impacts on the fate of a given VOI.

Material and methods

Patients

In this retrospective analysis of prospectively collected data, we included all stroke patients with acute perfusion CT (pCT) and follow-up MRI, treated by intravenous thrombolysis and/or endovascular therapy in our institution from 01 January 2016 to 31 December 2017. Exclusion criteria included poor-quality scans due to movement artifacts, contraindications to MRI, follow-up-MRI performed >10 days after onset as well as cerebral edema or hemorrhage causing major anatomical deformations. Recanalization was assessed in patients with endovascular treatment using the standardized Thrombolysis in Cerebral Infarction score (TICI).[5] TICI scores 2 b and 3 were considered as 'successful recanalization'. The study was conducted in accordance with the Helsinki declaration and was approved by the local ethics committee (Commission cantonale d'éthique de la recherche de Genève) which waived the requirement to obtain informed consent for this retrospective study.

Imaging acquisition

CT is performed as a standard of care in acute stroke patients admitted in our institution. Non-contrast head CT (NCCT), pCT and angio-CT (CTA) of the head and neck were acquired on the same Somatom Force CT (Siemens, Erlangen, Germany). pCT images were acquired after intravenous administration of 40 ml iodinated contrast at 5 ml/s by a power injector (Omnipaque, 350/40 ml, GE Healthcare, Chicago, USA). pCT imaging parameters were 80 kVp, 270 mAs, and 1.2-mm section collimation. Slice thickness was 5 mm. Four perfusion maps (CBF, CBV, MTT and Tmax) were calculated offline using standard software (RAPID, Ischemaview Stanford University, Stanford, USA).[6]

Follow-up MRI was performed on 1.5 T or 3.0 T machines (Siemens Prisma-fit 3 T, Siemens Skyra 3 T, Siemens Aera 1.5 T, Erlangen, Germany; Philips Ingenia 1.5 T, Best, Netherlands) as part of standard of care during hospitalization. The MRI protocol included diffusion-weighted imaging (DWI), T2-weighted and fluid-attenuated inversion recovery (FLAIR) sequences.

Infarct delineation

The final infarct was drawn manually on T2 images, with the help of DWI using MRIcron[7] by consensus of two board-certified stroke neurologists (ED, EC) blinded to acute perfusion maps. Based on the final infarct map, the outcome of each voxel was classified as infarcted (value 1) or non-infarcted (value 0).

Preprocessing

To compare perfusion maps (native CT space) and the final MRI-infarct mask (T2-MRI space) and allow voxelwise inference, all images were coregistered and normalized to a standardized MNI-CT space[8] using an in-house tool based on the normalized mutual information cost function as implemented in SPM12[9] for MATLAB (MathWorks, USA), as well as on tools from the FMRIB Software Library (FSLv.5).[10] In order to enhance the specificity of the models trained, a mask was applied to non-brain voxels in all data used for training, following a method for coarse cerebrospinal fluid segmentation described by Manniesing et al.[11]

As the collected dataset has a positive to negative ratio of 2:100 (number of infarcted voxels: number of non-infarcted voxels) after masking, all data used for training were undersampled using an in-house developed tool in Python (Python Software Foundation, v.3.6.5) to improve the learning process. This ensures that the final training datasets contain the same number of voxels originating from infarcted as from non-infarcted regions of the brain.[12] The distribution of infarcted voxels was left untouched in data used for testing.

General strategy

After coregistration of pCT maps and final infarct masks, the prediction of final infarction was estimated in a voxel-based approach using GLMs based on single perfusion maps (glm(MTT), glm(Tmax), glm(CBF)

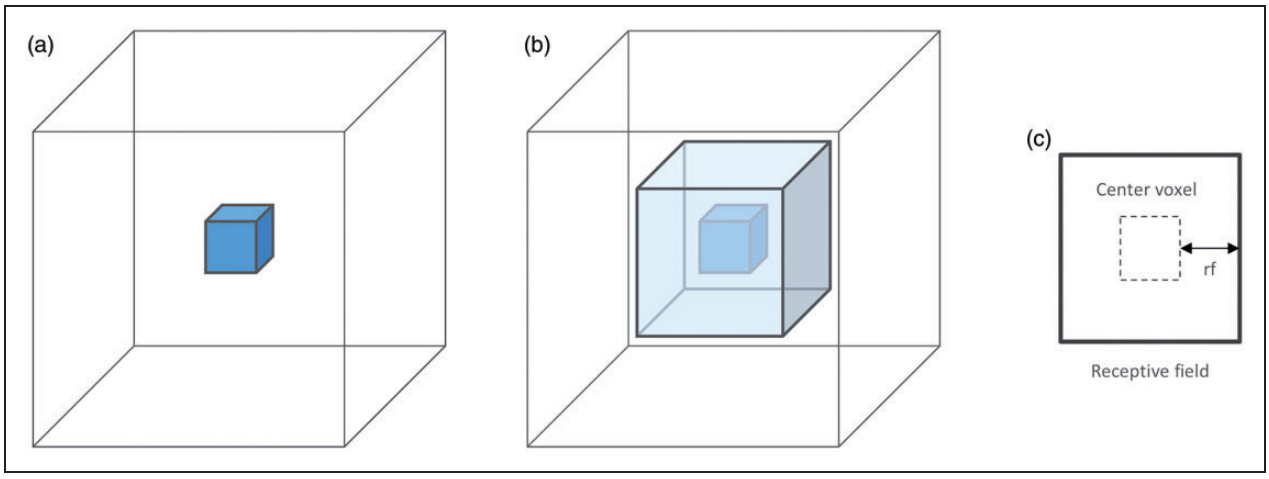

Figure 1. Schematic representation of a VOI and its receptive field. (a) A voxel-based model without receptive field evaluates the information contained in the VOI only ($2 \times 2 \times 2$ mm^3) (rf = 0). (b) A model using a 3D patch receptive field (light blue) includes information from neighboring voxels to the outcome of a given VOI. The size of the receptive field is defined as the number of voxels between the VOI and the outside boundary of the receptive field (c). For instance, a receptive field of size rf = 1 corresponds to a three-dimensional patch of size $3 \times 3 \times 3$ voxels ($6 \times 6 \times 6$ mm^3).

and glm(CBV)) and on all four perfusion parameters (glm(multi)). For each parameter-based model, receptive fields ranging in size from 0 ($rf = 0$) to 4 ($rf = 4$: $9 \times 9 \times 9$ voxels, i.e. $18 \times 18 \times 18\,\text{mm}^3$) were tested (Figure 1). We chose the GLM as the model to perform our analysis, as it remains one of the simplest models capable of multivariate analysis ensuring maximal reproducibility. We compared performance in patients who recanalized after treatment and in those who did not. In a post hoc analysis, because glm(Tmax) was the more accurate model in the above analysis, its performance to predict the final infarct was compared to the standard "non GLM" Tmax model.

General linear regression models. Generalized linear models are an extension of linear models that can be used in the setting of binary prediction problems. The classification of voxels can be seen as a binary variable P where the probability of tissue infarction is represented by the logistic function

$$P = \frac{1}{1 + e^{-f(x)}}$$

where $f(x)$ is the linear combination of one or more input parameters, grouped in an input vector $\boldsymbol{x}$

$$f(x) = \beta x + \alpha$$

where β is the model parametrization extracted from the training data and α is the intercept term. General linear models allow for multivariate analysis and can thus be used for the combination of different imaging modalities.[13] In this study, univariate (using MTT, Tmax, CBF and CBV independently) as well as multiparameter analysis (using all perfusion parameters combined) was applied to the classification of infarcted voxels. However, it can also be used to perform a multi-voxel analysis, using the values of voxels within the receptive field of the voxel to be predicted. In this setting, a new predictor function $f'(x_{i,j,k})$ can be defined such as

$$f'(x_{i,j,k}) = \alpha + \sum_{i-rf}^{i+rf} \sum_{j-rf}^{j+rf} \sum_{k-rf}^{k+\text{rf}} \beta_{i,j,k} x_{i,j,k}$$

where the log-odds of each voxel $x_{i,\,j,\,k}$ can be defined for each input parameter as the linear combination of all the voxels within a receptive field defined by the distance rf from the center voxel (see Figure 1). This can be used for models based on only one perfusion parameter, as well as on models relying on multiple modalities.

Receptive fields. We then examined whether performance of the same models was enhanced by integrating perfusion information from "receptive fields" that were implemented as concentric cubes of increasing volumes around an each VOI. The size of the receptive field (denoted rf) was defined as the number of voxels ($1\ \ voxel = 2 \times 2 \times 2\,\text{mm}^3$) between the VOI and the limits of the receptive field (Figure 1). To allow the use of a receptive field near the border of an image, all images were padded with null-value voxels accordingly. We evaluated models using cuboid RF ranging in

size from $rf = 0$ (equivalent to voxelwise prediction) to $rf = 4$ ($9 \times 9 \times 9$ $voxels = 18 \times 18 \times 18\,\mathrm{mm}^3$). The upper bound was dictated by the technical limit of our hardware, as all training data have to fit in random-access memory of the server the models are trained on.

Standard Tmax model (post hoc analysis). Tmax is commonly used to define regions at risk of infarction.[6,14–16] For comparison and validation, the performance of a non-GLM "standard model" Tmax without RF was estimated in a voxelwise approach. This model can be generalized as a function $g(T\mathrm{max})$ that is a normalized representation of the raw Tmax values which are mapped between 0 and 1 to represent probability of infarction.

$$g(T\mathrm{max}) = \frac{T\mathrm{max} - \min(T\mathrm{max})}{\max(T\mathrm{max}) - \min(T\mathrm{max})}$$

Smoothing kernels (post hoc analysis). Prior studies have shown that smoothing pCT images with a Gaussian blur can increase the signal-to-noise ratio and can thus improve the prediction of the infarct in acute stroke.[17] A spherically symmetric Gaussian kernel can be defined on R^N as the function $G_N(\vec{x};\ \sigma)$ of fixed width ω, where $\vec{x}\ \in R^N$ and $\sigma \in R$

$$G_N(\vec{x};\sigma) = \frac{1}{\left(\sqrt{2\pi}\sigma\right)^N} e^{-\frac{|\vec{x}|^2}{2\sigma^2}}$$

Two- and three-dimensional kernels were evaluated with an increasing kernel width ω and $\sigma = \frac{\omega}{3}$. For further comparison, the performance of non-GLM normalized perfusion parameters after Gaussian smoothing was evaluated in a voxelwise approach. The normalized representation of each perfusion parameter was estimated according to the formula described above.

Model evaluation. Cross-validation (CV) is an efficient way of assessing the performance as well as the generalizability of a model, while avoiding the bias that would occur if the model was validated on the data it was trained on. In repeated 5-fold patient-wise CV, 20% of patients are randomly chosen and held out from the training process for model evaluation for every fold. This process is repeated several times, and the median of all iterations is taken as the final performance. By iterating through the different possible patient combinations for training and testing, this technique ensures that the model is trained on, as well as tested on all the data without introducing bias. In this study, 5-fold patient-wise CV was repeated 10 times and the mean was taken as the final performance.

Model comparison. The area under the receiver operating characteristic (ROC) curve (AUC) was used to determine the efficiency of the different perfusion models to predict the final infarct.[18] The Dice coefficient[19] served as an additional metric to allow for better external comparability. This score measures the ratio between true positives (TP) and the sum of the volume of the prediction (true positive + false positive, TP + FP) and the volume of the ground truth (true positive + false negative, TP + FN). When all terms are null, the Dice coefficient is defined as 1.

$$Dice = \frac{2{*}TP}{(TP + FP) + (TP + FN)}$$

Model performance was then compared with the nonparametric Wilcoxon signed-rank test. Significance was defined at a standard level of $p < 0.05$.

Model performance in treatment option subgroups. To determine the influence of treatment options on model and perfusion marker performance, two subgroups were analyzed separately: patients benefitting from intravenous treatment (IVT) alone and patients benefitting from endovascular treatment (EVT) alone or in combination with IVT. The cross-validation protocol described previously was used in each subgroup. To compare the results between the two independent patient populations, a Mann–Whitney U test was used.

Results

Patients

One hundred forty-four patients (70 ± 16 years; 70 (49%) women) met the inclusion/exclusion criteria (see Supplementary Materials). Eighty patients received IVT alone, 24 EVT alone and 40 both. Median time from onset to CT was 130 min (IQR 81–220) and from onset to follow-up MRI 48 h (IQR 26–112). Patient characteristics are summarized in Table 1.

Contribution of cuboid receptive fields for final infarct prediction

Three representative patients are presented in Figure 2. This example shows that voxelwise predictions (Figure 2(b), $rf = 0$) tend to produce scattered risk maps when compared to models using RF (Figure 2(c) to (f)). The RF-based models generally outperformed voxelwise models in producing spatially coherent lesions and produced more accurate delineations of the lesion. Using RF as input, all five tested models demonstrated significantly higher performance for infarct prediction than single-voxel prediction based on AUC analysis, as

shown in Figure 3. Receptive fields of size $rf = 3$ performed best. For greater values of rf, performance did not statistically improve nor decrease. A RF of size $rf = 3$ was thus chosen as reference for all further comparisons. In terms of area under the ROC curve, applying receptive fields translated into a gain of 0.08 on average ($p < 0.01$, see Table 2 and Supplementary Materials). Compared to the standard (non-GLM)

Table 1. Patient characteristics ($n = 144$).

Age (years)	70±16
Sex (F)	70 (49)
NIHSS at admission	9 [4–15]
Time from onset to CT (minutes)	130 [81–220]
Time from onset to MRI (hours)	48 [26–112]
IVT only/EVT only/IVT+ EVT	80 (55)/24 (17)/40 (28)
Successful recanalization[a] (TICI 2b-3)	58 (90)
Final infarct volume (cm^3)	
EVT[a]	32.8 [8.9–64.7]
IVT only	4.6 [0.7–19.9]
Ischemic core volume[b] (cm^3)	
EVT[a]	10.0 [0.0–32.0]
IVT only	0.0 [0.0–5.8]
Ischemic penumbra volume[c] (cm^3)	
EVT[a]	135.0 [86.0–182.5]
IVT only	23.0 [4.0–55.0]

Note: Data are presented as median [25–75 IQR], mean ± SD and N (%).
[a]Assessed in patients with EVT ($n = 64$).
[b]Defined as CBF < 30%, as assessed by the RAPID software.
[c]Defined as Tmax > 6 s, as assessed by the RAPID software.

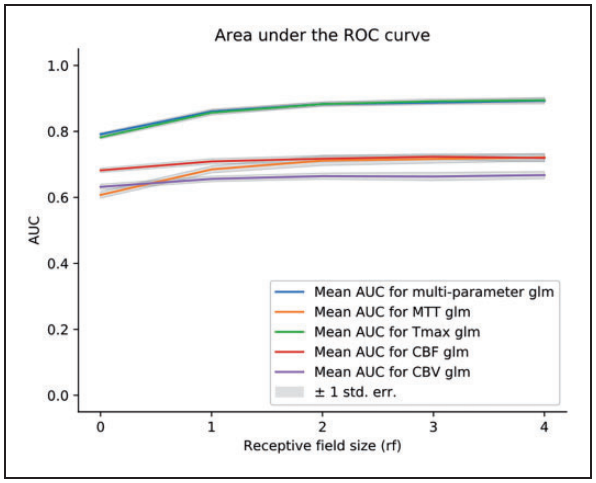

Figure 3. Performance of the models with receptive fields of increasing size. Performance expressed as mean AUC for: rf = 0 (no receptive field); rf = 1 $6 \times 6 \times 6$ mm^3; rf = 2 $10 \times 10 \times 10$ mm^3 rf = 3 $14 \times 14 \times 14$ mm^3 rf = 4 $18 \times 18 \times 18$ mm^3.

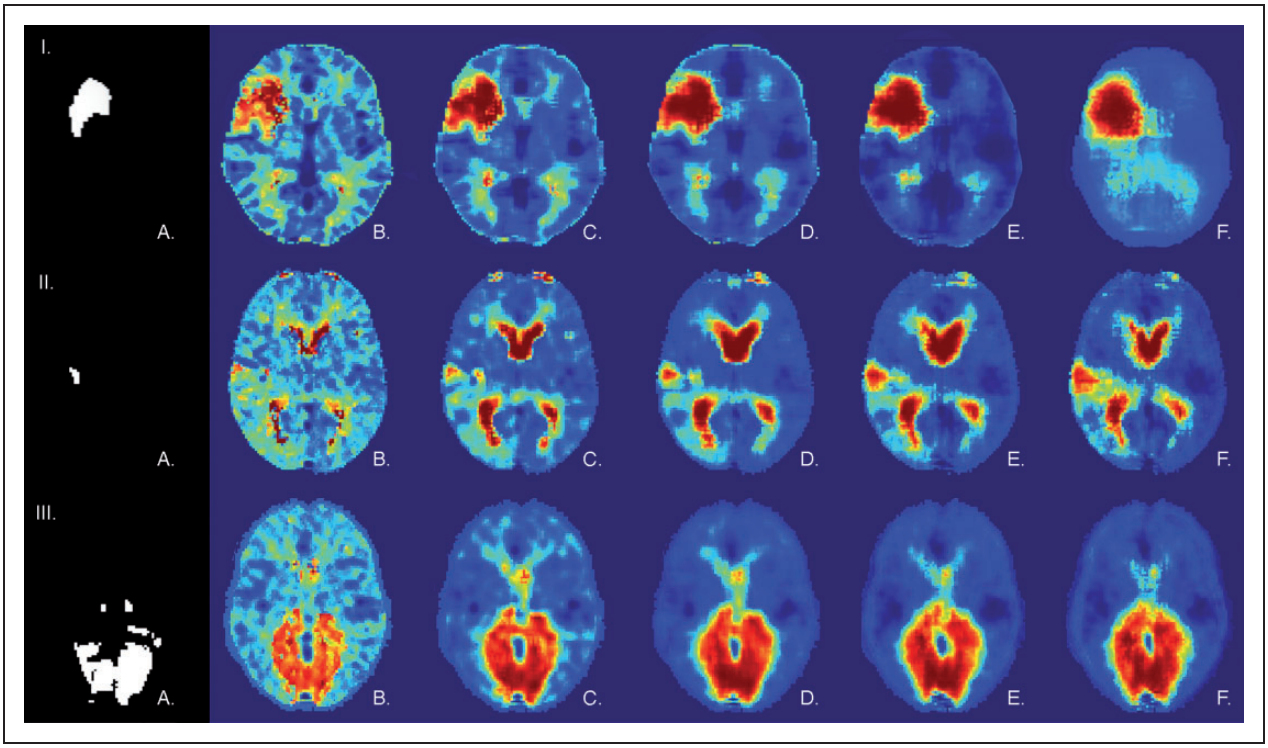

Figure 2. Examples of infarct prediction with receptive fields of increasing size. (I to III) Illustration of infarct prediction for three representative patients from a cross-validation test set. (I) A right moderate size middle cerebral circulation infarct treated by IVT alone. (II) A right small size posterior cortical middle cerebral artery infarct treated by IVT alone. (III) A bilateral posterior cerebral artery stroke treated by EVT. For every patient: (a) Lesion mask delineated on follow-up MRI. (b to f) Probability of infarction maps as predicted by the multi-modal GLM model (glm(multi)) with a receptive field varying in size from $rf = 0$ (voxelwise prediction) to $rf = 4$. No mask was applied to this data.

Table 2. Performance of the different models to predict the final infarct.

	No receptive field ($rf = 0$ $2 \times 2 \times 2$ mm^3 VOI)		Receptive field ($rf = 3$ $14 \times 14 \times 14$ mm^3)		p-values	
Model	AUC	Dice	AUC	Dice	AUC	Dice
GLM models						
glm(CBV)	0.63	0.046	0.66	0.050	<10e-4	> 0.05
glm(CBF)	0.68	0.053	0.72	0.061	<10e-6	<0.05
glm(MTT)	0.61	0.051	0.72	0.076	<10e-9	<10e-9
glm(Tmax)	0.78	0.115	0.89	0.157	<10e-9	<10e-10
glm(multi)	0.79	0.115	0.89	0.155	<10e-9	<10e-10
Tmax Models						
g(Tmax)	0.78	0.030	/	/	/	/

Table 3. Performance of voxelwise models after 3D Gaussian smoothing and models with a receptive field to predict the final infarct.

3D Gaussian smoothing ($rf = 0$ $2 \times 2 \times 2$ mm^3 VOI)			Receptive field ($rf = 3$ $14 \times 14 \times 14$ mm^3)		
Model	Best kernel width (mm)	AUC	Model	AUC	p-values
g(CBF)	10	0.70	glm(CBF)	0.72	<0.01
g(CBV)	14	0.64	glm(CBV)	0.66	0.03
g(MTT)	38	0.65	glm(MTT)	0.72	<10e-6
g(Tmax)	22	0.85	glm(Tmax)	0.89	<10e-6

Tmax model (AUC 0.78 ± 0.03), glm(Tmax) performed statistically better only when using RF (glm(Tmax) AUC 0.89 ± 0.03 with RF; $p < 0.01$; glm(Tmax) AUC 0.78 ± 0.02 without RF; $p > 0.05$). After iterating over 2D and 3D smoothing kernels with increasing width, the optimal smoothing kernel was determined for every parameter (see Supplementary Materials). When comparing optimized Gaussian smoothing to the use of RF, RF models performed significantly better for all perfusion parameters ($p < 0.05$; Table 3). Duration of data processing of our RF-based models did not exceed a few seconds and would not therefore delay acute therapy (see Supplementary Materials, Table 3).

Comparison between perfusion parameters for final infarct prediction

As shown in Figure 4 and Table 2, Tmax is the best single parameter to predict the final infarct with and without RF ($p < 0.01$). No significant difference could be found between Tmax and multiparameter models ($p > 0.05$). glm(Tmax) also led to the highest gain of AUC with a mean increase of 0.11 ($p < 0.01$), followed by glm(MTT), glm(multi), glm(CBF) and glm(CBV) when applying a RF of size $rf = 3$. At a voxelwise level, the analysis of the mean weights applied by the glm(multi) model showed that Tmax and CBF were attributed significantly more importance than MTT and CBV ($p < 0.05$). There were no glm(Tmax) AUC differences between patients who recanalized and those who did not (0.89 vs. 0.86; $p > 0.05$).

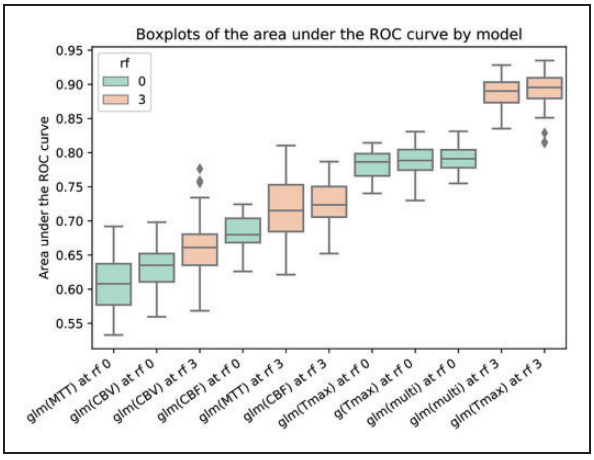

Figure 4. Comparison of the performance of the different models to predict the final infarct. Boxplots for the predictive models ordered by AUC value. Receptive fields of size rf = 0 (shown in green) and rf = 3 (shown in orange) were used. g (Tmax) represents the standard (non-glm) model. Each box extends from the 25th percentile to the 75th percentile with a line indicating the median. Upper and lower whiskers show the range up to the upper and lower extreme (±1.5*inter-quartile range). Outliers are represented by grey diamond shapes.

Comparison between EVT and IVT subgroups

A treatment subgroup analysis was performed on 64 patients that had received EVT either alone or in combination with IVT and on 80 patients that had benefitted from IVT alone (see Table 4 in Supplementary Materials). In terms of AUC, no significant difference

could be found for the glm(CBV), glm(CBF) and glm (multi) models ($p > 0.05$). For MTT and Tmax, the glm model performed better on the IVT subgroup ($p < 10e\text{-}5$ and $p = 0.04$ respectively). Interestingly, the standard non-GLM Tmax model performed significantly better in the IVT subgroup ($p < 10e\text{-}5$). Intra-group analysis is reported in the Supplementary Materials.

Discussion

Our results suggest that, in acute stroke patients, the fate of a predefined hypoperfused region is more accurately predicted when taking into account the perfusion pattern of the surrounding tissue (i.e. in the receptive field). When tested on cross-validation data, model performance with receptive fields was higher than that of simple voxelwise models for all perfusion parameters. The glm(Tmax) and the glm(multi), which combines all four perfusion parameters (CBF, CBV, MTT and Tmax), showed the highest performance in predicting the final infarct.

Model performance of the different GLMs increased significantly with the use of receptive fields, highlighting the importance of spatially resolved information contained in CT-based perfusion imaging data. These findings held true in both the IVT and the EVT subgroup. In other words, fate prediction for one VOI was improved by taking into account perfusion data of neighboring voxels. For glm(Tmax), the use of receptive fields increased the performance from fair (AUC = 0.78) to good-excellent (AUC = 0.89). These results are consistent with biological concepts of brain ischemia, which suggests that neighboring regions that share the same vascular supply and collateral flow display a comparable risk of infarction. Model performance increased significantly with receptive fields including the nearest neighbors but plateaued with receptive fields of larger volumes. It can even be expected that information from distant voxels would provide divergent information that may decrease model performance in predicting the fate of the VOI. Our results based on perfusion CT are consistent with preliminary MRI studies using regional information from perfusion and diffusion imaging in human and mice.[1,20]

In the current study, we used a RF of cuboid shape. Individually shaped receptive fields may increase the performance of the model.[21] The use of receptive fields improved the prediction of infarcted tissue, but it also seemed to enhance resistance to noise of a model, as confirmed by visual inspection. The concept of integrating information from spatially related voxels to decrease noise is also present in Gaussian kernel smoothing, as used in earlier models.[17] Gaussian smoothing can be seen as a special case of receptive fields where the weights are arranged following a Gaussian function along every dimension. However, the receptive field models trained on the dataset outperforms models relying on optimized Gaussian smoothing alone. As the trained weights of the receptive fields can hold a representation of the directionality of the signal within a kernel, they offer an advantage over smoothing relying on a Gaussian function. Moreover, as receptive fields do not presuppose a constant weight distribution, they can be regionally finetuned to integrate the spatial infarct probability distribution in future imagewise models. Receptive fields are an inherent feature of convolutional neural networks and may explain the encouraging results reported by recent studies using this method.[2,22,23] Although our findings emphasize the need for further development in the field, receptive fields can already be applied to enhance the performance of currently employed models.

Comparison of the different models showed that glm (Tmax) as well as a linear combination of all perfusion parameters glm(multi) performed best to predict the final infarct with a good to excellent accuracy (AUC = 0.89). This performance, based on imaging data only relying on the regional information provided by RF, was similar to the accuracy reported in a previous GLM study, which included clinical data in addition to imaging data, without RF.[24] It was also comparable to earlier studies using non-linear models that included diffusion (DWI) in addition to perfusion MRI.[20] Interestingly, our model for infarct prediction reached a similar AUC as more sophisticated gradient-boosted tree models such as XGBoost.[25]

Among all perfusion parameters, we found Tmax to be the most valuable to predict the final infarct. This is reflected in the performance of the glm(Tmax) model but also in the weight of the Tmax variable in the multi-parametric glm(multi). CBF also significantly contributed to the performance of the glm(multi) model. Interestingly, in the IVT subgroup, both g (Tmax) and glm(MTT) performed slightly better than in the EVT subgroup. In a previous multi-modal study, Tmax and MTT but not CBF were the most informative perfusion parameters.[26] The differences in performance of the individual perfusion parameters between centers suggest that the analysis of perfusion imaging remains difficult and may be the result of variations in the generation of perfusion maps. Nevertheless, our results suggest that Tmax may be the most reliable parameter to predict the final infarct with pCT. As the multimodal model glm(multi) performs just as well, it may also be considered and could prove better at palliating the variations stemming from the generation of perfusion maps.

Limitations of this study include the analysis of imaging data of patients from a single center.

However, the standardized perfusion output obtained from the RAPID software package ensures a better reproducibility and limit differences in the model analysis before validation. The influence of reperfusion status on the prediction of infarction could not be evaluated in our study as only a small fraction of patients had a documented unsuccessful recanalization. We were therefore unable to determine which perfusion parameter performed better depending on the recanalization status.[27,28] No clinical outcome was considered in our study, as the goal of this study was to develop new tools to enhance current infarct prediction methods for patient stratification at the acute stage. Further studies are nevertheless needed to investigate the added value of clinical data to these models.

Our findings support a multidimensional approach, integrating both perfusion and spatial parameters. Receptive fields inform a given model about the state of adjacent tissue, allowing it to outperform purely voxelwise generalized linear models. Our model of spatial receptive fields does not require any manual input nor thresholding and can be easily applied to predictive models already used in a clinical setting. Receptive fields are easy to implement and effective tools to improve the prediction of the final infarct and guide patient's selection for acute stroke treatment.

Funding

The author(s) disclosed receipt of the following financial support for the research, authorship, and/or publication of this article: Emmanuel Carrera and Dimitri Van De Ville received support from the Swiss Heart Foundation. Maria G Preti received support from the Center for Biomedical Imaging (CIBM) of the Geneva-Lausanne Universities and the EPFL.

Acknowledgements

We acknowledge Mathilde Fargeat and Damien Schneider for collecting the data used in the manuscript, as well as Simon Narduzzi for reviewing the algorithms used for the predictive models.

Declaration of conflicting interests

The author(s) declared no potential conflicts of interest with respect to the research, authorship, and/or publication of this article.

Authors' contributions

Julian Klug: study concept and design, algorithm design and implementation, data acquisition, statistical analysis, interpretation of data, manuscript. Elisabeth Dirren: data acquisition, final infarct delineation, interpretation of data. Maria Giulia Preti: algorithm design, critical revision of manuscript. Paolo Machi: data acquisition. Andreas Kleinschmidt: study guidance. Maria Isabel Vargas: data acquisition and data processing. Dimitri Van De Ville: algorithm design, study concept and design. Emmanuel Carrera: study concept and design, interpretation of data, critical revision of manuscript.

Supplemental material

Supplemental material for this article is available online.

ORCID iDs

Julian Klug https://orcid.org/0000-0002-4849-9811
Emmanuel Carrera https://orcid.org/0000-0003-0045-5382

References

1. Huang S, Shen Q and Duong TQ. Artificial neural network prediction of ischemic tissue fate in acute stroke imaging. *J Cereb Blood Flow Metab* 2010; 30: 1661–1670.
2. Nielsen A, Hansen MB, Tietze A, et al. Prediction of tissue outcome and assessment of treatment effect in acute ischemic stroke using deep learning. *Stroke* 2018; 49: 1394–1401.
3. Sherrington CS. *The integrative action of the nervous system*. New Haven: Yale University Press, 1906.
4. Hubel DH and Wiesel TN. Receptive fields of single neurones in the cat's striate cortex. *J Physiol* 1959; 148: 574–591.
5. Higashida RT, Furlan AJ, Roberts H, et al. Trial design and reporting standards for intra-arterial cerebral thrombolysis for acute ischemic stroke. *Stroke* 2003; 34: e109–137.
6. Straka M, Albers GW and Bammer R. Real-time diffusion-perfusion mismatch analysis in acute stroke. *J Magn Reson Imaging* 2010; 32: 1024–1037.
7. Rorden C and Brett M. Stereotaxic display of brain lesions. *Behav Neurol* 2000; 12: 191–200.
8. Rorden C, Bonilha L, Fridriksson J, et al. Age-specific CT and MRI templates for spatial normalization. *Neuroimage* 2012; 61: 957–965.
9. Friston K. CHAPTER 2 – statistical parametric mapping. In: Friston K, Ashburner J, Kiebel S, et al. (eds) *Statistical parametric mapping*. London: Academic Press, 2007, pp.10–31.
10. Woolrich MW, Jbabdi S, Patenaude B, et al. Bayesian analysis of neuroimaging data in FSL. *Neuroimage* 2009; 45(1 Suppl): S173–186.
11. Manniesing R, Oei MTH, Oostveen LJ, et al. White matter and gray matter segmentation in 4D computed tomography. *Sci Rep* 2017; 7: 119.
12. Jonsdottir K, Østergaard L and Mouridsen K. Predicting tissue outcome from acute stroke magnetic resonance imaging. *Stroke* 2009; 40: 3006–3011.
13. Wu O, Koroshetz WJ, Ostergaard L, et al. Predicting tissue outcome in acute human cerebral ischemia using combined diffusion- and perfusion-weighted MR imaging. *Stroke* 2001; 32: 933–942.
14. Olivot J-M, Mlynash M, Zaharchuk G, et al. Perfusion MRI (Tmax and MTT) correlation with xenon CT cerebral blood flow in stroke patients. *Neurology* 2009; 72: 1140–1145.

15. Olivot J-M, Mlynash M, Thijs VN, et al. Optimal Tmax threshold for predicting penumbral tissue in acute stroke. *Stroke* 2009; 40: 469–475.
16. Christensen S, Mouridsen K, Wu O, et al. Comparison of 10 perfusion MRI parameters in 97 sub-6-hour stroke patients using voxel-based receiver operating characteristics analysis. *Stroke* 2009; 40: 2055–2061.
17. Campbell BC, Christensen S, Levi CR, et al. Cerebral blood flow is the optimal CT perfusion parameter for assessing infarct core. *Stroke* 2011; 42: 3435–3440.
18. Hanley JA and McNeil BJ. The meaning and use of the area under a receiver operating characteristic (ROC) curve. *Radiology* 1982; 143: 29–36.
19. Dice LR. Measures of the amount of ecologic association between species. *Ecology* 1945; 26: 297–302.
20. Scalzo F, Hao Q, Alger JR, et al. Regional prediction of tissue fate in acute ischemic stroke. *Ann Biomed Eng* 2012; 40: 2177–2187.
21. Frindel C, Rouanet A, Giacalone M, et al. Validity of shape as a predictive biomarker of final infarct volume in acute ischemic stroke. *Stroke* 2015; 46: 976–981.
22. Stier N, Vincent N, Liebeskind D, et al. Deep learning of tissue fate features in acute ischemic stroke. *Proc IEEE Int Conf Bioinform Biomed* 2015; 2015: 1316–1321.
23. Pinto A, Mckinley R, Alves V, et al. Stroke lesion outcome prediction based on MRI imaging combined with clinical information. *Front Neurol* 2018; 9: 1060.
24. Kemmling A, Flottmann F, Forkert ND, et al. Multivariate dynamic prediction of ischemic infarction and tissue salvage as a function of time and degree of recanalization. *J Cereb Blood Flow Metab* 2015; 35: 1397–1405.
25. Livne M, Boldsen JK, Mikkelsen IK, et al. boosted tree model reforms multimodal magnetic resonance imaging infarct prediction in acute stroke. *Stroke* 2018; 49: 912–918.
26. Livne M, Kossen T, Madai VI, et al. Multiparametric model for penumbral flow prediction in acute stroke. *Stroke* 2017; 48: 1849–1854.
27. d'Esterre CD, Boesen ME, Ahn SH, et al. Time-dependent computed tomographic perfusion thresholds for patients with acute ischemic stroke. *Stroke* 2015; 46: 3390–3397.
28. Wintermark M, Flanders AE, Velthuis B, et al. Perfusion-CT assessment of infarct core and penumbra: receiver operating characteristic curve analysis in 130 patients suspected of acute hemispheric stroke. *Stroke* 2006; 37: 979–985.